Ultrasonic cavitation bubble- and gas bubble-assisted fractional precipitation for the purification of (+)-dihydromyricetin

Jieun Hong and Jin-Hyun Kim[†]

Center for Future Sustainable Technology, Department of Chemical Engineering,
Kongju National University, Cheonan 31080, Korea

Abstract–This study presents the ultrasonic cavitation bubble- and gas bubble-assisted fractional precipitation that dramatically improves the precipitation efficiency in existing precipitation method for purifying (+)-dihydromyricetin. Compared to the conventional method, the time required for precipitation was reduced by 40 times. The particle size was reduced by 4.0-7.4 times and 3.7-4.4 times for cavitation bubbles and gas bubbles, respectively, and the diffusion coefficient was increased by 5.1-9.2 times (cavitation bubble) and 3.7-4.4 times (gas bubble). Meanwhile, the precipitation rate constant was increased by 11.0-65.0 times and 17.0-24.6 times and the activation energy was decreased by $-5,543 \sim -9,655$ J/mol and $-6,546 \sim -7,404$ J/mol, which resulted in an improved precipitation rate. The results of the thermodynamic analysis showed that the precipitation was exothermic and non-spontaneous.

Keywords: (+)-Dihydromyricetin, Fractional Precipitation, Ultrasonic Cavitation Bubble, Gas Bubble, Mechanism

INTRODUCTION

Ampelopsis grossedentata is a medicinal plant which contains large amounts of flavonoids [1]. In particular, (+)-dihydromyricetin ((+)-ampelopsin) (Fig. 1) is a major functional flavonoid and a bioactive component found in large quantities in the leaves of *A. grossedentata* [2]. It is a functional substance excellent for not only hangover relief and liver protection, but also for the treatment of inflammation, fatty liver disease, cancers, diabetes, and hyperlipidemia. Therefore, it is widely used as a raw material for foods and pharmaceuticals [1-3]. Du et al. [4] reported that (+)-dihydromyricetin derived from *A. grossdentata* greatly restricted hypertension. Yoshikawa et al. [5] also reported that it promoted muscle relaxation through in vivo metabolism of ethanol and had an anti-allergy effect.

Fractional precipitation is a simple and effective method to purify (+)-dihydromyricetin using solubility differences. The process, which

Fig. 1. The chemical structure of (+)-dihydromyricetin.

[†]To whom correspondence should be addressed.
E-mail: jinhyun@kongju.ac.kr

was developed in 2008, allows for high purity (>83.2%) (+)-dihydromyricetin to be obtained. However, it took a long time (~32 h) for fractional precipitation, which limited its implementation for mass production [6]. To resolve this limitation, a method was developed to improve the precipitation efficiency by increasing the surface area per volume of the reaction solution by introducing an ion exchange resin (Amberlite 200, Amberlite IR 120Na) in 2014 [7]. Introducing Amberlite 200 to the reaction solution achieved a high yield (>90%) of (+)-dihydromyricetin in a relatively short time (~16 h). Nonetheless, problems still existed because of the ion exchange cost and difficulty recovering the ion exchange after precipitation with surface area-increasing materials. Furthermore, the long fractional precipitation time of (+)-dihydromyricetin and the feasibility of mass production still remain unsolved. Accordingly, there is a high demand for a method to drastically shorten the precipitation time and allow for effective mass production of (+)-dihydromyricetin through fractional precipitation. Recently, various studies have been conducted to improve the precipitation efficiency (especially shortening the precipitation time) due to an increase in the nucleation rate by ultrasound [8-10]. In 2021, fractional precipitation using ultrasound remarkably improved the purification efficiency of (+)-dihydromyricetin. The precipitation time required to obtain (+)-dihydromyricetin with high purity (87.01-91.66%) and yield (90.63-92.00%) was reduced by 40 times (~30 min) through ultrasound-induced fractional precipitation (ultrasonic power: 80-250 W) compared to the conventional method (~1,200 min) [11]. This improvement was due to acoustic cavitation, the formation, growth, and collapse of microbubbles, in the liquid irradiated by ultrasound. When the cavitation bubbles formed by the ultrasound finally collapse, they create high-speed microjets of solution, intense localized heating, and high-pressure shock waves in the solution, which ultimately improves the micro-mixing, mass transfer, and supersaturation of the solution [12]. Studies on the clear mechanism of ultra-
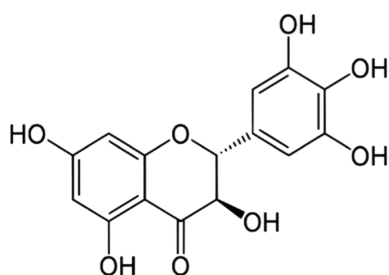
sound-assisted precipitation are insufficient and no studies about the mechanism of fractional precipitation of (+)-dihydromyricetin by ultrasound have been conducted. Therefore, this study investigated in detail the ultrasound-precipitation mechanism by introducing ultrasonic cavitation bubbles and gas bubbles during fractional precipitation. Ultrasonic cavitation bubbles expand and collapse resulting in high-speed microjets, intense localized heating, and high-pressure shock waves, whereas gas bubbles only expand during their lifetime, so high temperatures and pressures are not generated [13]. Based on these differences in characteristics, we investigated the precipitation mechanism by observing the precipitation behavior of (+)-dihydromyricetin in fractional precipitation using ultrasonic cavitation bubbles and gas bubbles. In addition, the diffusion pattern of molecules was quantitatively identified by determining the diffusion coefficient using the Stokes-Einstein equation. Furthermore, the characteristics of ultrasound-fractional precipitation were investigated through a kinetic analysis using the Johnson-Mehl-Avrami-Kolmogorov (JMAK) equation and through a thermodynamics analysis using the Arrhenius, van't Hoff, and Eyring equations.

MATERIALS AND METHODS

1. (+)-Dihydromyricetin Samples

In this study, the samples [crude extract (purity: 54.84%)] used for fractional precipitation of (+)-dihydromyricetin were procured from Guilin Natural Ingredient, Inc. (Guilin, China).

2. Fractional Precipitation

The schematic diagrams of the ultrasonic cavitation bubble- and gas bubble-induced fractional precipitation using the solubility difference of (+)-dihydromyricetin in acetone solution are presented in Fig. 2. (+)-Dihydromyricetin (purity: 54.84%) was dissolved in acetone (0.1 g/mL). Then the solution was added dropwise into the distilled water-acetone solution (ratio=5/1, v/v) while stirring (335 rpm), and the precipitation of (+)-dihydromyricetin using solubility difference was induced [3,7]. The volume of the reactor was set to be 20 mL and the working volume was set to 12 mL during the fractional precipitation. The ultrasound-fractional precipitation was initiated in an ultrasonic bath at 5 °C while varying the ultrasonic power (80, 180, 250, 380, and 540 W) and precipitation time (5, 10, 20, and 30 min). For the thermodynamic analysis of the ultrasound-fractional precipitation, another precipitation was performed at 15 °C and 25 °C using the same method. Ultrasonic power of 180 W was found to be optimal and was adopted for the precipitation process. To investigate the mechanism of ultrasound-fractional precipitation further, ultrasonic cavitation bubbles were replaced with gas bubbles and injected into the precipitation solution using a gassing unit (SH-A2, Amazonpet, Korea) equipped with air stone (pore diameter: 10 μm). The effects of gas flow rate (0.185, 0.65, and 1.75 L/min) through the gassing unit on the efficiency of the fractional precipitation (precipitation time, yield, and purity) were investigated. The (+)-dihydromyricetin precipitate was then obtained after filtering (150 mm, Whatman, Buckinghamshire, UK) and the precipitate was dried in a vacuum oven (UP-2000, EYELA, Japan) at 40 °C for 24 h. The purity and yield of the dried precipitate were determined through HPLC.
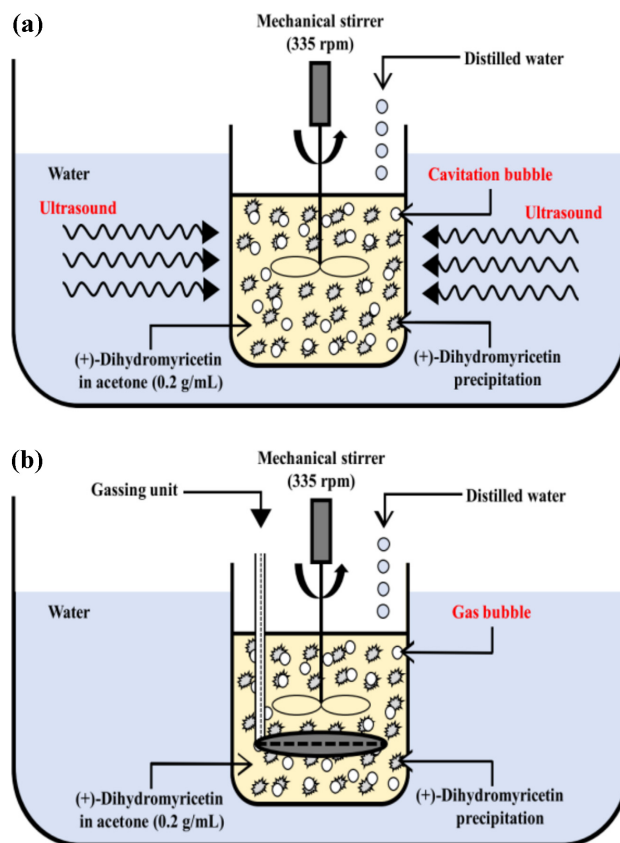
Fig. 2. Schematic diagram of ultrasonic cavitation bubble-assisted fractional precipitation (a) and gas bubble-assisted fractional precipitation (b) for the purification of (+)-dihydromyricetin.

3. (+)-Dihydromyricetin Analysis

(+)-Dihydromyricetin was analyzed through an HPLC system (SCL-10 AVP, Shimadzu, Japan). A mobile phase of 0.1% trifluoroacetic acid/acetonitrile 90/10 (v/v) flowed for 5 min under the gradient condition and then the flow was changed to 30/70 (v/v) for 30 min. The flow rate was set to 1.0 mL/min, and 20 μL of the sample was injected and analyzed at UV 254 nm [3]. For the analysis, an authentic sample (purity: 98%) was purchased from Guilin Natural Ingredient, Inc. (Guilin, China) [11].

4. Size Measurement of Precipitate

The morphology and size of the precipitate obtained from the fractional precipitation were measured through an electron microscope (SV-35 Video Microscope System, Some Tech, Korea) [7]. The precipitate was analyzed under high magnification (×200) and the size of the precipitate was measured from video images using IT-Plus System (Some Tech, Korea) [11].

5. Estimation of Diffusion Coefficient

The diffusion coefficient of the (+)-dihydromyricetin molecules (B) diffused in the fractional precipitation solvent (A) was calculated from the Stokes-Einstein equation and can be expressed as Eq. (1) [10]:

$$D_{AB} = \frac{kT}{6\pi r_0 \eta} \tag{1}$$

where k is the Boltzmann constant (1.38×10^{-23} J/K), r_0 is the molec-

ular diameter of (+)-dihydromyricetin, η is the dynamic viscosity of the solution, and T is the absolute temperature of the solution. The solution viscosity was measured with a viscometer (Viscolite 700, Hydromotion, UK) [11].

6. Kinetic Analysis

The Johnson-Mehl-Avrami-Kolmogorov (JMAK) equation is mainly used in the crystallization or precipitation process to investigate isothermal phase-transformation kinetics during nucleation and growth, and it is expressed as Eq. (2) and Eq. (3) [8,14,15]:

$$X(t) = 1 - \exp[-kt^n] \tag{2}$$

$$\log\left\{\ln\left[\frac{1}{1-X(t)}\right]\right\} = n\log t + \log k \tag{3}$$

where X(t) is composed of the precipitation yield of (+)-dihydromyricetin at t, k is the precipitate rate constant, and n is the Avrami index that describes the crystal structure and the characteristics of nucleation. The JMAK index (Avrami index) n and rate constant k can be calculated from the slope and intercept using Eq. (3).

7. Thermodynamic Analysis

The activation energy (E_a, kJ/mol) refers to the minimum energy required for a reaction and can be calculated using the Arrhenius equation. It is expressed as Eq. (4) [15].

$$\ln k = \ln A - \frac{E_a}{RT} \tag{4}$$

where k is the precipitation rate constant, k_0 is the frequency factor, T is the absolute temperature of the solution, and R is the gas constant (8.314 J/mol·K).

Activation parameters, such as the activation enthalpy change (ΔH^*, kJ/mol), activation entropy change (ΔS^*, J/mol·K), and activation Gibbs energy change (ΔG^*, kJ/mol), were used to investigate the thermodynamic changes in the transition state of the precipitation reaction. ΔH^* and ΔS^* were calculated with the Eyring equation, Eq. (5), and ΔG^* was calculated with Eq. (6) [15]:

$$\frac{\ln k}{T} = \ln\frac{k_B}{h} + \frac{\Delta S^*}{R} - \frac{\Delta H^*}{RT} \tag{5}$$

$$\Delta G^* = \Delta H^* - T\Delta S^* \tag{6}$$

where k is the rate constant calculated from the JMAK equation. In addition, k_B is the Boltzmann constant (1.38×10^{-23} J/K), h is the Planck constant (6.6261×10^{-34} J·s), T is the absolute temperature, and R is the gas constant (8.314 J/mol·K).

Thermodynamic parameters, such as the standard enthalpy change (ΔH^o, kJ/mol), standard entropy change (ΔS^o, J/mol·K), and standard Gibbs energy change (ΔG^o, J/mol), were calculated to evaluate the spontaneity, feasibility, and nature of the precipitation process. ΔH^o, ΔS^o, and ΔG^o can be calculated from the following equations [15]:

$$\Delta G^o = -RT\ln K_e \tag{7}$$

$$\ln K_e = -\frac{\Delta H^o}{RT} + \frac{\Delta S^o}{R} \tag{8}$$

where K_e is the equilibrium constant, which is the concentration ratio between the (+)-dihydromyricetin remaining in the superna-
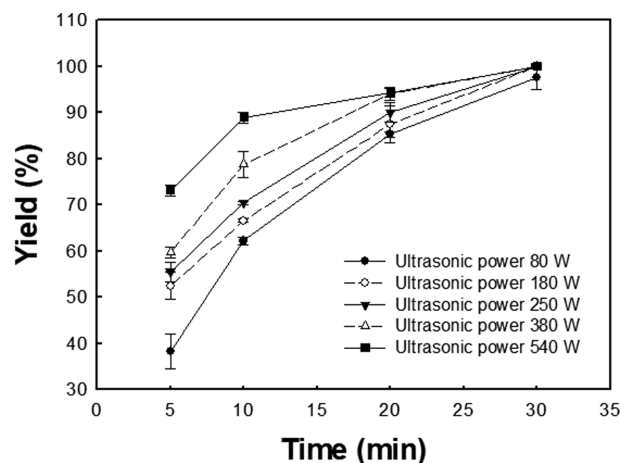

Fig. 3. Effect of ultrasonic power on the yield of (+)-dihydromyricetin obtained by ultrasonic cavitation bubble-assisted fractional precipitation at 5 °C.

tant and the precipitated (+)-dihydromyricetin.

RESULTS AND DISCUSSION

1. Ultrasonic Cavitation Bubble-assisted Fractional Precipitation

Fractional precipitation is a pre-purification process that can simply and efficiently purify (+)-dihydromyricetin by using solubility differences. However, conventional fractional precipitation takes a long time, which is not economically feasible for the mass production of (+)-dihydromyricetin [11]. To improve this issue, ultrasound (power: 80-540 W) was introduced to the fractional precipitation of (+)-dihydromyricetin. The yields from the fractional precipitation of (+)-dihydromyricetin according to the ultrasonic power are presented in Fig. 3. The yield from the conventional fractional precipitation of (+)-dihydromyricetin very slowly increased with time, and the precipitation completed in 1,200 min (yield: 88.7%) [11]. On the other hand, the yield from the ultrasound-fractional precipitation of (+)-dihydromyricetin sharply increased with the precipitation time under all ultrasonic powers (80-540 W), and almost all of the (+)-dihydromyricetin was recovered within a 30 min precipitation time. In particular, the (+)-dihydromyricetin yield was over 99% with ultrasonic powers higher than 180 W during the 30 min precipitation time. The ultrasound-fractional precipitation not only remarkably improved the yield but also considerably shortened the precipitation time by about 40 times compared to the conventional fractional precipitation. In addition, a highly pure (+)-dihydromyricetin (82.54-91.12%) was obtained under the ultrasonic power of 80 to 540 W (data not shown).

2. Gas Bubble-assisted Fractional Precipitation

To explain the reason for the improvement of the efficiency (shortening the precipitation time) in ultrasound-fractional precipitation, it was investigated whether the effect of the bubble itself generated by the ultrasonic wave or the effect of the bubble collapse [16,17]. Gas bubbles were introduced instead of ultrasonic cavitation bubbles during the fractional precipitation. Unlike ultrasonic cavitation bubbles, gas bubbles only expand during their lifetime, so they will not generate high-speed microjets, intense localized
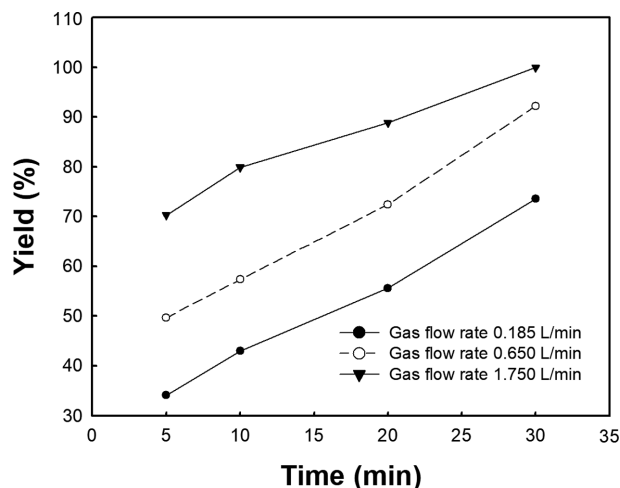
Fig. 4. Effect of gas flow rate on the yield of (+)-dihydromyricetin obtained by gas bubble-assisted fractional precipitation at 5 °C.

heating, and high-pressure shock waves [18]. In this study, fractional precipitation was performed by introducing different gas flow rates (0.185, 0.65, and 1.75 L/min). The fractional precipitation results according to the gas flow rates are presented in Fig. 4. The (+)-dihydromyricetin yields increased with all the gas flow rates as the precipitation time elapsed, and most of the (+)-dihydromyricetin (>99%) could be recovered at the gas flow rate of 1.75 L/min in a precipitation time of 30 min. The purity of (+)-dihydromyricetin under the gas flow rate condition of 0.185 to 1.75 L/min was 69.70 to 81.94% (data not shown). In short, the gas bubble-fractional precipitation could also remarkably shorten the precipita-

tion time compared to the conventional fractional precipitation. The obtained results were similar to those obtained with ultrasound-fractional precipitation, implying that the roles of the ultrasonic cavitation bubbles and gas bubbles were similar during the fractional precipitation. Even though the ultrasonic cavitation bubbles and gas bubbles have different characteristics, the precipitation times were significantly reduced in both ultrasound-fractional precipitation and gas bubble-fractional precipitation. Therefore, fractional precipitation with ultrasonic cavitation bubbles and gas bubbles introduced might enhance the precipitation rate because the bubbles themselves act as sites for heterogeneous nucleation, thus lowering the free energy barrier required for nucleation and promoting precipitation as shown in Fig. 5 [18]. Finally, in the case of the ultrasonic cavitation bubble, the bubble itself has more significant impact on the fractional precipitation than the effect of the bubble collapse (high-pressure shock waves, high-speed microjets, intense localized heating, etc.).

3. Determination of Diffusion Coefficient of (+)-Dihydromyricetin in Solution

To investigate the characteristics of fractional precipitation more quantitatively, the particle sizes r_0 were measured in the precipitates of the ultrasound-fractional precipitation and the gas bubble-fractional precipitation using an electron microscope. The results are arranged in Table 1. The solution viscosities for conventional fractional precipitation, fractional precipitation using cavitation bubbles, and precipitation using gas bubbles were measured to be 1.0 g/cm·s, 0.8 g/cm·s, and 1.0 g/cm·s, respectively, and the viscosity did not change dramatically during precipitation. The mean particle size until the precipitation completion was 68.587 µm for the conventional precipitation. Whereas, the mean particle sizes of the
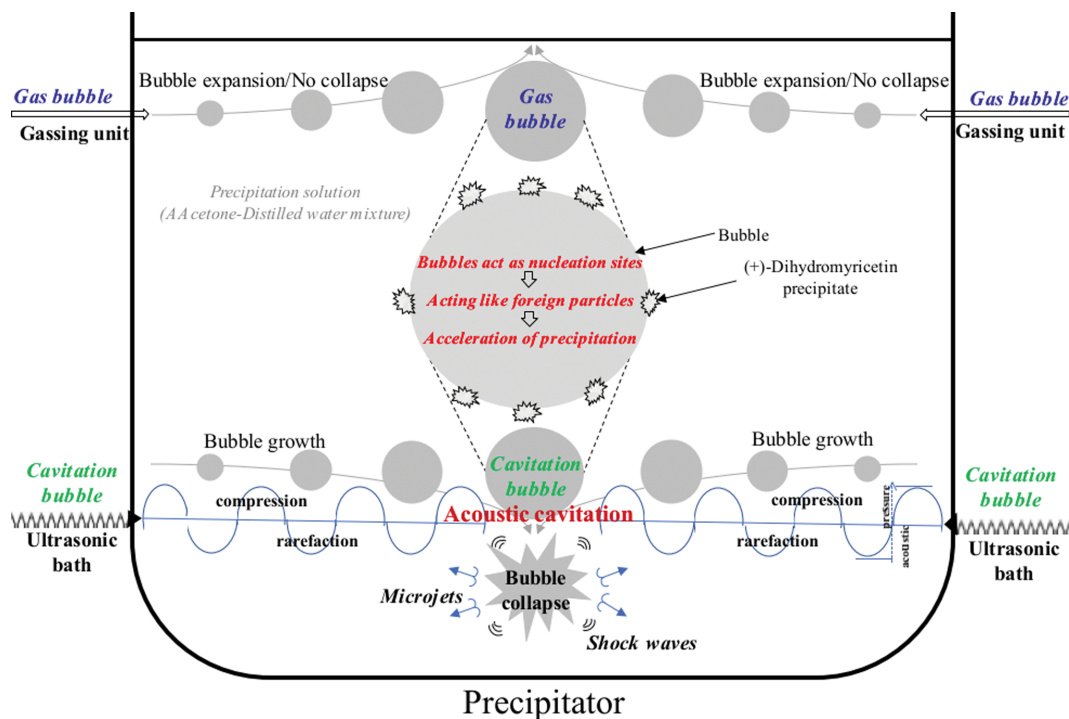

Fig. 5. A proposed mechanism for ultrasonic cavitation bubble- and gas bubble-assisted fractional precipitation of (+)-dihydromyricetin.

Table 1. Effect of ultrasonic cavitation bubbles and gas bubbles on viscosity, mean particle size and diffusion coefficient at 5 °C

Fractional precipitation type	Ultrasonic power (W)	Gas flow rate (L/min)	Viscosity η (cp)	Mean particle size r_0 (μm)	Diffusion coefficient D_{AB} (cm^2/s)
Control*	-	-	1.0	68.587	2.9701×10^{-11}
With ultrasonic cavitation bubble	80		0.8	16.963	1.5006×10^{-10}
	180		0.8	15.251	1.6690×10^{-10}
	250	-	0.8	14.884	1.7102×10^{-10}
	380		0.8	11.897	2.1396×10^{-10}
	540		0.8	9.292	2.7394×10^{-10}
With gas bubble	-	0.185	1.0	18.727	1.0874×10^{-10}
		0.65	1.0	16.196	1.2573×10^{-10}
		1.75	1.0	15.758	1.2923×10^{-10}

*Conventional fractional precipitation

ultrasound-fractional precipitations were 16.963 (80 W), 15.251 (180 W), 14.884 (250 W), 11.897 (380 W), and 9.292 μm (540 W), meaning the particles were 4.0 to 7.4 times smaller than the particles of the conventional fractional precipitation. As the ultrasonic power increased, the particle size decreased. The decrement originates from the shock waves and the abrasion between the particles when ultrasonic power is introduced [16,19]. In general, a reduced particle size in an active pharmaceutical ingredient not only improves the dissolution rate, uniformity of drug dispersion, and oral bioavailability during formulation, but also improves the drying efficiency [20,21]. Therefore, reducing the (+)-dihydromyricetin particle size is very important for its usage. In the case of the gas bubble-fractional precipitation, the mean particle sizes were 18.727 μm (0.185 L/min), 16.196 μm (0.65 L/min), and 15.758 μm (1.75 L/min), 3.7 to 4.4 times smaller than those of the conventional fractional precipitation. Similar to the ultrasound-fractional precipitation, as the gas flow rate increased, the mean particle size decreased further. The diffusion coefficient D_{AB} was calculated using the Stokes-Einstein equation to find the diffusion behavior of the fractional precipitation methods (Table 1). The D_{AB} of the conventional fractional precipitation was 2.9701×10^{-11} cm^2/s [11]. On the other hand, ultrasound-fractional precipitation had D_{AB} values of

1.5006×10^{-10} (80 W), 1.6690×10^{-10} (180 W), 1.7102×10^{-10} (250 W), 2.1396×10^{-10} (380 W), and 2.7394×10^{-10} cm^2/s (540 W), 5.1 to 9.2 times higher than that of the conventional fractional precipitation. In addition, the gas bubble-fractional precipitation had D_{AB} values of 1.0874×10^{-10} (0.185 L/min), 1.2573×10^{-10} (0.65 L/min), and 1.2923×10^{-10} cm^2/s (1.75 L/min), 3.7 to 4.4 times higher than that of the conventional precipitation. An increased diffusion coefficient in a fractional precipitation greatly affects the homogeneous nucleation [10,22,23]. It was clear from the D_{AB} values that both the ultrasonic cavitation bubbles and the gas bubbles affected the diffusion during the precipitation. Additionally, the ultrasonic cavitation bubbles within the ultrasonic power range of 80 to 540 W affected the fractional precipitation more than the gas bubbles at gas flow rates of 0.185 to 1.75 L/min. This might be attributed to the effect of hotspots, microjets, and shock waves caused by the collapse of the cavitation bubbles [9,10,24]. As the diffusion coefficient increased, the mass transfer between molecules was facilitated, leading to easier precipitation and improved precipitation efficiency [10,11].

4. Kinetic Analysis

Kinetic analysis was performed for the fractional precipitation of (+)-dihydromyricetin at 5 °C with ultrasonic cavitation bubbles and gas bubbles by applying the experimental data of Fig. 3 and

Table 2. Values of kinetic parameters for the fractional precipitation of (+)-dihydromyricetin at different ultrasonic powers and gas flow rates at 5 °C

Fractional precipitation type	Ultrasonic power (W)	Gas flow rate (L/min)	n (-)	k (-)	ΔE_a** (J/mol)	r^2 (-)
Control*	-	-	0.7431	0.0085	-	0.8272
With ultrasonic cavitation bubble	80		0.9941	0.0934	−5,543	0.9886
	180		0.7410	0.2164	−7,486	0.9805
	250	-	0.8145	0.2329	−7,656	0.9852
	380		0.8195	0.2405	−7,730	0.9987
	540		0.5637	0.5528	−9,655	0.9680
With gas bubble	-	0.185	0.6180	0.1441	−6,546	0.9492
	-	0.65	0.6901	0.1988	−7,290	0.8846
	-	1.75	0.9730	0.2089	−7,404	0.7487

*Conventional fractional precipitation

**$\Delta E_a = E_{a, \text{ultrasonic cavitation bubble or gas bubble}} - E_{a, \text{control}}$

Fig. 4 to the JMAK equation. That is, $\log\left\{\ln\left[\dfrac{1}{1-X(t)}\right]\right\}$ versus log t was plotted using Eq. (3). Then the JMAK factor (n) and the rate constant (k) were determined from the slope and intercept. These values are presented in Table 2. For the conventional fractional precipitation, k was 0.0085, and n was 0.7431 [11]. Whereas, for the ultrasound-fractional precipitation (80-540 W) and the gas bubble-fractional precipitation (0.185-1.75 L/min), the k values were 0.0934 to 0.5528 and 0.1441 to 0.2089, and the n values were 0.5637 to 9941 and 0.6180 to 0.9730, respectively. The k values increased by 11.0 to 65.0 times in the ultrasound-fractional precipitation and 17.0 to 24.6 times in the gas bubble-fractional precipitation compared to the conventional fractional precipitation. The activation energy changes ΔE_a ($E_{a, ultrasonic\ cavitation\ bubble\ or\ gas\ bubble} - E_{a, control}$) according to the Arrhenius equation were $-5{,}543$ (80 W), $-7{,}486$ (180 W), $-7{,}656$ (250 W), $-7{,}730$ (380 W), and $-9{,}655$ J/mol (540 W) in the ultrasound-fractional precipitation. Meanwhile, the activation energy changes for the gas bubble-fractional precipitation were $-6{,}546$ (0.185 L/min), $-7{,}290$ (0.65 L/min), and $-7{,}404$ J/mol (1.75 L/min). Therefore, the activation energy was reduced by introducing ultrasonic cavitation bubbles and gas bubbles. In addition, as the ultrasonic power and gas flow rate increased, the activation energy decreased further. As a conclusion, introducing ultrasonic power and gas bubbles could decrease the activation energy and improve the precipitation rate. The results are similar to those obtained in the fractional precipitation of paclitaxel where ultrasonic power was introduced [8].

5. Thermodynamic Analysis

A fractional precipitation was conducted for (+)-dihydromyricetin with the ultrasonic power of 180 W and varying temperatures (5, 15, and 25 °C). To carry out the thermodynamic studies, the minimum ultrasonic power (180 W) to obtain a yield greater than 99% was adopted considering precipitation efficiency (Fig. 6). The yields were 100% (5 °C), 84.17% (15 °C), and 69.71% (25 °C) during the 30 min precipitation time. The lower the precipitation temperature, the higher the precipitation yield. The highest precipitation efficiency for (+)-dihydromyricetin could be achieved at the ultrasonic power of 180 W and at 5 °C. Meanwhile, in order to investigate the thermodynamic changes in the transition state, ΔH^* and ΔS^* were determined. The rate constant k, which was obtained from each applied temperature through the JMAK equation, was applied in the Eyring equation in Eq. (5). ΔG^* was determined through Eq. (6) (Table 3). ΔH^* was a negative value (-12.799 kJ/mol), which meant that the precipitation was exothermic, and ΔS^* was also negative (-226.272 J/mol·K), meaning that the precipitation included an associative mechanism [25,26]. The ΔG^* values were 50.158
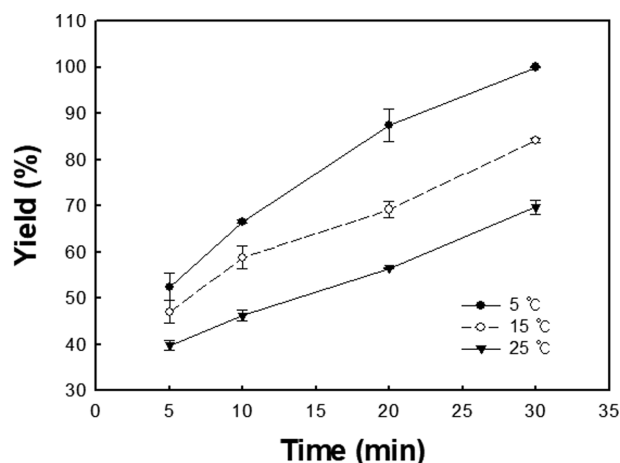

Fig. 6. Effect of temperature on the yield of (+)-dihydromyricetin obtained by ultrasonic cavitation bubble-assisted fractional precipitation at 180 W.

(5 °C), 52.420 (15 °C), and 54.683 kJ/mol (25 °C), which were all positive and they increased as the precipitation temperature increased. This means that the reactions were nonspontaneous, thus additional energy was required [25]. The thermodynamic parameters such as ΔH^o, ΔS^o, and ΔG^o obtained through the van't Hoff equation in Eq. (7) and Eq. (8) are presented in Table 3. The K_e values were 0.875 (5 °C), 0.855 (15 °C), and 0.697 (25 °C), which decreased as the precipitation temperature increased. This trend was because E_a was negative (-10.385 kJ/mol); thus, the precipitation became more active at a lower temperature. The ΔH^o was negative (-7.753 kJ/mol) and exothermic and ΔS^o was also negative (-28.732 J/mol·K) as shown in Table 3, indicating that randomness or disorder was reduced during the precipitation process. Furthermore, the ΔG^o values increased to 0.309 (5 °C), 0.375 (15 °C), and 0.894 kJ/mol (25 °C) according to the temperature increase, and the precipitation was non-spontaneous as the values were all positive [15].

CONCLUSIONS

The purification efficiency of (+)-dihydromyricetin was dramatically improved by ultrasonic cavitation bubble- and gas bubble-assisted fractional precipitation. The precipitation time was reduced by 40 times compared to the existing precipitation method. As a result of examining the precipitation mechanism, it was found that the bubble itself acts as a nucleation site, resulting in faster nucleation and thereby improving precipitation efficiency. The yield of (+)-dihydromyricetin increased as the precipitation temperature

Table 3. Values of activation parameters and thermodynamic parameters for the ultrasonic cavitation bubble-assisted fractional precipitation of (+)-dihydromyricetin at different temperatures

Temperature (°C)	K_e (-)	E_a (kJ/mol)	$\Delta H^*/\Delta H^o$ (kJ/mol)	$\Delta S^*/\Delta S^o$ (J/mol·K)	$\Delta G^*/\Delta G^o$ (kJ/mol)
5	0.875				50.158/0.309
15	0.855	-10.385	$-12.799/-7.753$	$-226.272/-28.732$	52.420/0.375
25	0.697				54.683/0.894

(5-25 °C) decreased, the ultrasonic power (80-540 W) and gas flow rate (0.185-1.75 L/min) increased. In addition, compared to the conventional method, the particle size was reduced by 4.0-7.4 times (cavitation bubbles) and 3.7-4.4 times (gas bubbles) and the diffusion coefficient increased by 5.1-9.2 times (cavitation bubbles) and 3.7-4.4 times (gas bubbles), indicating that these bubbles also affect the homogeneous nucleation in a solution. Furthermore, the precipitation rate constant was increased by 11.0-65.0 times and 17.0-24.6 times and the activation energy was decreased by −5,543~ −9,655 J/mol and −6,546~−7,404 J/mol, which resulted in an improved precipitation rate. The thermodynamic parameters ΔH^o, ΔS^o, and ΔG^o were negative (−7.753 kJ/mol), negative (−28.732 J/mol·K), and positive (0.309-0.894 kJ/mol at 5-25 °C), respectively, revealing the exothermic and non-spontaneous nature of the precipitation.

ACKNOWLEDGEMENTS

REFERENCES

1. X. J. Zheng, H. Xiao, Z. Zeng, Z. W. Sun, C. Lei, J. Z. Dong and Y. Wang, *J. Funct. Foods*, **9**, 290 (2014).
2. F. Li, A. Raza, Y.-W. Wang, X.-Q. Xu and G.-H. Chen, *Phcog. Mag.*, **13**, 446 (2017).
3. S. B. Ji and J. H. Kim, *Korean J. Chem. Eng. Res.*, **56**, 370 (2018).
4. Q. Du, W. Cai, M. Xia and Y. Ito, *J. Chromatogr. A*, **973**, 217 (2002).
5. M. Yohsikawa and T. Murakami, *Chem. Pharm. Bull.*, **44**, 1736 (1996).
6. K. H. Lee and J. H. Kim, *Biotechnol. Bioprocess Eng.*, **13**, 274 (2008).
7. M. K. Lim and J. H. Kim, *Korean J. Microbiol. Bioteachnol.*, **42**, 25 (2014).
8. H. W. Seo and J. H. Kim, *Process Biochem.*, **87**, 238 (2019).
9. B. S. Schueller and R. T. Yang, *Ind. Eng. Chem. Res.*, **40**, 4912 (2001).
10. S. V. Dalvi and R. N. Dave, *Int. J. Pharm.*, **387**, 172 (2010).
11. S. R. Oh and J. H. Kim, *Korean J. Chem. Eng.*, **38**, 480 (2021).
12. J. Jordens, N. D. Coker, B. Gielen, T. V. Gerven and L. Braeken, *Ultrason. Sonochem.*, **26**, 64 (2015).
13. H. J. Kang and J. H. Kim. *Process Biochem.*, **99**, 316 (2020).
14. C. G. Lee and J. H. Kim, *Process Biochem.*, **59**, 216 (2017).
15. J. N. Park and J. H. Kim, *Process Biochem.*, **53**, 224 (2017).
16. K. Wohlgemuth, F. Ruether and G. Schembecker, *Chem. Eng. Sci.*, **65**, 1016 (2010).
17. H. S. Min and J. H. Kim, *Korean J. Chem. Eng.*, **39**, 58 (2022).
18. K. Wohlgemuth, A. Kordylla, F. Ruether and G. Schembecker, *Chem. Eng. Sci.*, **64**, 4155 (2009).
19. Z. Guo, M. Zhang, H. Li, J. Wang and E. Kougoulos, *J. Cryst. Growth*, **273**, 555 (2005).
20. P. Khadka, J. Ro, H. Kim, I. Kim, J. T. Kim, H. Kim, J. M. Cho, G. Yun and J. Lee, *Asian J. Pharm. Sci.*, **9**, 304 (2014).
21. M. J. Kim and J. H. Kim, *Korean J. Chem. Eng. Res.*, **54**, 278 (2016).
22. D. Ma, J. S. Marshall and J. Wu, *J. Acoust. Soc. Am.*, **114**, 3496 (2018).
23. Z. Guo, A. G. Jones and N. Li, *Chem. Eng. Sci.*, **61**, 1617 (2008).
24. L. Wolloch and J. Kost, *J. Control. Release*, **148**, 204 (2010).
25. T. H. Yoon and J. H. Kim, *Biotechnol. Bioprocess Eng.*, **25**, 777 (2020).
26. A. L. Petrou and A. Terzidaki, *Chem. Geol.*, **381**, 144 (2014).